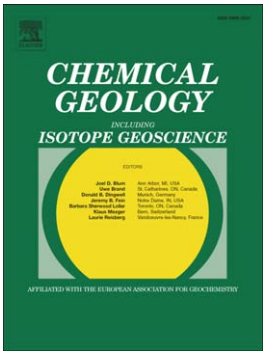

A new test for equilibrium based on clinopyroxene-melt pairs: Clues on the solidification temperatures of Etnean alkaline melts at post-eruptive conditions

Silvio Mollo, Keith Putirka, Valeria Misiti, Michele Soligo, Piergiorgio Scarlato

PII: S0009-2541(13)00232-5
DOI: doi: 10.1016/j.chemgeo.2013.05.026
Reference: CHEMGE 16896

To appear in: *Chemical Geology*

Received date: 21 February 2013
Revised date: 4 May 2013
Accepted date: 25 May 2013

Please cite this article as: Mollo, Silvio, Putirka, Keith, Misiti, Valeria, Soligo, Michele, Scarlato, Piergiorgio, A new test for equilibrium based on clinopyroxene-melt pairs: Clues on the solidification temperatures of Etnean alkaline melts at post-eruptive conditions, *Chemical Geology* (2013), doi: 10.1016/j.chemgeo.2013.05.026

A new test for equilibrium based on clinopyroxene-melt pairs: Clues on the solidification temperatures of Etnean alkaline melts at post-eruptive conditions

Silvio Mollo[1], Keith Putirka[2], Valeria Misiti[1], Michele Soligo[3], and Piergiorgio Scarlato[1]

[1] Istituto Nazionale di Geofisica e Vulcanologia, Via di Vigna Murata 605, 00143 Roma, Italy

[2] California State University, Fresno, Department of Earth and Environmental Sciences, 2576 E. San Ramon Avenue, MS/ST25, Fresno, California 93740-8039, U.S.A.

[3] Dipartimento di Scienze Geologiche, Università "Roma Tre", Largo San Leonardo Murialdo 1, 00146 Roma, Italy

Running title: A new test for equilibrium based on clinopyroxene-melt pairs

Corresponding author:

Dr. Silvio Mollo

Istituto Nazionale di Geofisica e Vulcanologia

Via di Vigna Murata 605

00143 Roma - ITALY

office tel. +39 0651860674

lab tel. +39 0651860223

fax +39 0651860507

ABSTRACT

We have performed new global regression analyses to calibrate a model of equilibrium between clinopyroxene and co-existing melt. Then we have applied this model to a restricted but important range of clinopyroxene and melt compositions from Mt. Etna volcano. The degree of disequilibrium is determined through the comparison between components "predicted" for clinopyroxene via regression analyses of clinopyroxene-liquid pairs in equilibrium conditions, with those "measured" in the analyzed crystals. The model is tested using compositions not included into the calibration dataset, i.e., clinopyroxene-melt pairs obtained from equilibrium and cooling rate experiments conducted at ambient pressure on an Etnean trachybasalt. The experiments were duplicated at the NNO+1.5 and QFM oxygen buffering conditions estimated for magmas at Mt. Etna. Both equilibrium and disequilibrium clinopyroxene-melt pairs from the experiments were also used as input data for one of the most recent thermometers based on the Jd-DiHd exchange reaction. Results from calculations indicate that, under rapid cooling rate conditions, clinopyroxenes do not equilibrate with the melt. Consequently, the thermometers predict higher crystallization temperatures compared to the final experimental temperature, prior to rapid quenching of the experiment. The systematic difference between expected and measured compositions and temperatures allows us to calibrate a model that describes undercooling based on disequilibrium exchange reactions. We use this new tool to estimate the thermal history of naturally cooled lava flows and dikes at Mt. Etna volcano.

Keywords: clinopyroxene; cooling rate; test for equilibrium; thermometer

1. INTRODUCTION

Clinopyroxenes are widespread in igneous rocks and their compositions are routinely used for elucidating magma storage conditions (e.g., Putirka 2008). Petrologists often use the Fe-Mg exchange between clinopyroxene and melt [$^{cpx\text{-}melt}Kd_{Fe\text{-}Mg} = (Fe^{cpx}/Fe^{melt}) \times (Mg^{melt}/Mg^{cpx})$] to ascertain whether the clinopyroxene-melt pairs chosen for the estimate of magmatic temperatures were in equilibrium at the time of crystallization. This practice has a long history for both olivine and clinopyroxene; authors have indeed suggested that, at the equilibrium condition, $^{ol\text{-}melt}Kd_{Fe\text{-}Mg}$ and $^{cpx\text{-}melt}Kd_{Fe\text{-}Mg}$ yield constant values of 0.30±0.02 (Roeder and Emslie 1970; Matzen et al. 2011) and 0.27±0.03 (Grove and Bryan 1983; Sisson and Grove 1993; Putirka et al. 2003), respectively. However, it has also long been know that Fe-Mg exchange has certain limitations. For example, Gee and Sack (1988) highlighted that $^{olivine\text{-}melt}Kd_{Fe\text{-}Mg}$ is sensitive to melt composition, which implies that fixed values for such coefficients cannot be applied. Similarly, Putirka (2008) showed that $^{cpx\text{-}melt}Kd_{Fe\text{-}Mg}$ is not a reliable indicator of clinopyroxene-liquid equilibrium for a wide range of compositions. It is important, therefore, to employ a range of tests of equilibrium, whenever possible, such as by comparing "predicted" *versus* "measured" mineral components. In fact, authors investigating the influence of kinetic effects on olivine and clinopyroxene compositions have highlighted that crystal-melt pairs from disequilibrium experiments yield values for both $^{ol\text{-}melt}Kd_{Fe\text{-}Mg}$ and $^{cpx\text{-}melt}Kd_{Fe\text{-}Mg}$ (Baker and Grove 1985; Conte et al. 2006; Mollo et al. 2010, 2012) that match those derived from isothermal experiments.

To augment the tools currently available, we re-examine some existing models that may be applied as tests of equilibrium, and derive a new model that can be used under disequilibrium conditions to assess undercooling of magmas at Mt. Etna volcano. Our approach takes advantage of the fact than clinopyroxenes do not re-equilibrate with the melt under rapid growth conditions, which allows kinetic or time-dependent pathways of a natural

system to be "frozen-in". To this end, we have performed new global regression analysis that improves upon one of the models that test for equilibrium, as presented in Putirka (1999). This model has been then tested using clinopyroxene-melt pairs obtained from equilibrium and cooling rate experiments conducted on an Etnean trachybasalt. In order to reproduce the solidification path of clinopyroxene microphenocrysts at post-eruptive conditions, the experiments were conducted at ambient pressure and oxygen fugacities comparable to those estimated for Etnean lavas (e.g., Lanzafame et al. 2013; Mollo et al., 2013a). Clinopyroxene-melt pairs from this study have been also used as input data for one of the most recent thermometers reported by Putirka (2008). Results demonstrate that in a given cooling rate experiment, clinopyroxenes record successively higher temperatures as the rate of cooling is increased. Although previous cooling rate studies suggested that rapidly cooled clinopyroxenes give rise to unreliable temperature estimations (e.g., Mollo et al. 2010), new experimental data indicate that model temperature estimates are positively correlated with the difference between the saturation temperature of clinopyroxene for a given Etnean liquid, and the final solidification temperature of the system (i.e., before final rapid quenching). On this basis, we are able to calibrate a new tool for estimating the thermal path of naturally cooled lava flows and dikes at Mt. Etna volcano, a model that should be applicable to similar alkaline compositions.

2. THE CASE STUDY OF MT. ETNA VOLCANO

Mt. Etna volcano is the largest sub-aerial volcano in Europe, and one of the most active and intensely monitored on Earth. Over the last 300 kyrs, Mt. Etna emitted abundant trachybasalt to basaltic trachyandesite to trachyandesite lavas, mainly characterized by the ubiquitous occurrence of clinopyroxene, plagioclase and titanomagnetite (Tanguy et al. 1997). Petrological and geophysical studies have attested that intratelluric crystals generally form at

500-100 MPa and 1200-1000 °C with melt-water contents of 1-2 wt.% (Metrich and Clocchiatti 1989; Corsaro et al. 1996, 2009; Bonaccorso et al. 2010; Viccaro et al. 2006; Del Gaudio et al. 2010; Mollo et al. 2011a, 2011b, 2011c; Armienti et al. 2012; Heap et al. 2013). Mineral and glass compositions from lava flows and dikes also record variable redox states of the liquid from NNO+1.5 to QFM (Metrich and Rutherford 1999; Mollo et al. 2011a, 2013a; Lanzafame et al. 2013). Some lava flows exhibit *pahoehoe* morphologies as the result of a low phenocryst content (<15 vol.%) during magma rising to the surface (Lanzafame et al. 2013; Mollo et al. 2013a). These lava flows crystallize after eruption, consequently, microphenocrysts typically form at ambient pressure conditions over variable cooling rates (e.g. Cashman 1993; Hammer 2008; Mollo et al. 2011a; 2011b). Textural and compositional data of *pahoehoe* lava flows from Mt. Etna volcano suggest, indeed, that crystals with a size <1 mm solidified at post-eruptive conditions, during or after lava emplacement (Lanzafame et al. 2013).

On the basis of (i) numerical simulations of thermal regimes in and around magmatic intrusions (Mollo et al. 2011a), (ii) geospeedometry measurements (Mollo et al. 2013b), (iii) and crystal compositional changes (Mollo et al. 2011a), it has been determined that lava flows and dikes from Mt. Etna volcano solidify at cooling rates ranging from 0.12 to 480 °C/h. This broad variation of three orders of magnitude matches with the thermal path determined for lava flows from other volcanic complexes, e.g. Tenerife, Kenya and Hawaii (Ujike 1982; Wilding et al. 1995; Gottsmann et al. 2004; Del Gaudio et al. 2010 and references therein). Moreover, rapidly cooled clinopyroxene microphenocrysts from Etnean melts are frequently enriched in Al, Na and Ti resembling those observed in previous dynamic crystallization studies and in variably cooled basic volcanic rocks (Smith and Lindsley 1971; Mevel and Vende 1976; Grove and Bence 1977, 1979; Grove and Raudsepp 1978; Coish and Taylor 1979; Gamble and Taylor 1980; Uijke 1982; Baker and Grove 1985; Faraone et al. 1988;

Lofgren et al. 2006; Baginski et al. 2009; Latypov et al. 2011; Mollo et al. 2010, 2011a, 2011b, 2012). This means that, during solidification of lava flows and dikes, clinopyroxene crystals form over an ever-changing temperature comprised between the liquidus and final temperature of the crystal growth. In this view, Mt. Etna volcano is a natural laboratory where the final composition of the crystals strictly depends on the thermal path experienced by magmas at post-eruption conditions.

3. EXPERIMENTS AND ANALYSES

The synthesis of the starting material, the isothermal and cooling rate experiments and the chemical analyses described in this study were carried out at the HP-HT Laboratory of Experimental Volcanology and Geophysics of the Istituto Nazionale di Geofisica e Vulcanologia in Rome (Italy).

3.1 Experimental techniques

The starting composition used in this study is a Holocene alkali basalt from Mt. Etna volcano (Sicily, Italy) characterized by the occurrence of clinopyroxene as its liquidus phase at about 1200 °C (Tanguy et al. 1997; Del Gaudio et al. 2010). Approximately 50 g of rock were reduced to a homogeneous powder in a ball mill. The resulting mixture was ground so as to pass through a #200 mesh sieve and then melted. The glass was powdered, sieved and melted for a second time to ensure the homogeneity of the final starting material. Melting experiments were conducted in a Fe pre-saturated Pt-crucible (see Conte et al. 2006 for further details) loaded in 1-atm furnace at 1600 °C for 1 hour; the sample was inserted directly into the furnace at 1600 °C and then quenched in a water bath. The glass was analyzed by X-ray powder diffraction and scanning electron microscopy and no crystalline phases were detected. Twenty electron microprobe analyses of this glass yielded an almost

homogeneous composition (in wt.%) of SiO_2=49.71 (±0.33), TiO_2=1.43 (±0.05), Al_2O_3=15.34 (±0.18), FeO=8.61 (±0.11), MnO=0.16 (±0.01), MgO=7.04 (±0.12), CaO=11.54 (±0.15), Na_2O=3.84 (±0.08), K_2O=1.40 (±0.04), P_2O_5=0.40 (±0.03), Cr_2O_3=0.03 (±0.01).

Ambient pressure experiments were performed in a vertical tube gas-mixing furnace. Fe pre-saturated Pt-capsules (see Conte et al. 2006 for further details) loaded with the starting powder were suspended within the furnace in an atmosphere of CO/CO_2 gas mixture. Oxygen fugacity was monitored and maintained constant over the experimental temperatures by means of an yttria-doped-zirconia solid electrolyte oxygen sensor ($SIRO_2$, Ceramic Oxide Fabricators, Ltd., Australia) and two digital thermal mass flow meters controlled via software. Following Tormey et al. (1987), the experiments were performed under a partial pressure of sodium (in the form of Na_2SiO_3) in the furnace atmosphere to minimize the sodium loss in the melt. All the experiments were duplicated using two different buffering conditions, i.e. the nickel-nickel oxide plus 1.5 (NNO+1.5) and the quartz-fayalite-magnetite (QFM) buffer. They can be divided into two sets (Table 1). Experimental Set 1 was carried out in order to assess the composition of clinopyroxene at the equilibrium condition. The samples were heated at a rate of 35 °C/min from room temperature up to 1200 ° and 1100 °C, holding the final temperature constant for 72 hours (i.e. isothermal experiments). Since cooling rate is the main process leading to the solidification of magmas, Experimental Set 2 was designed to quantify systematic changes in clinopyroxene and melt composition under disequilibrium conditions (i.e. cooling rate experiments). The samples were cooled using three cooling rates of 2.5 °, 10 ° and 50 °C/h from 1250 ° down to 1100 °C and then immediately quenched. A superliquidus temperature (1250 °C) was reached starting from room temperature (with a heating ramp of 100 °C/min) and it was maintained for 30 minutes before beginning cooling. Each experiment was rapidly quenched by dropping the charge into a water bath. The run product was mounted in epoxy and a polished thin section was produced from the epoxy

block.

3.2 Analytical techniques

Chemical analyses were carried out with an Electronic Probe Micro Analysis (EPMA) Jeol-JXA8200 combined EDS-WDS (five spectrometers with twelve crystals). For glasses, a slightly defocused electronic beam with a size of 3 μm was used with a counting time of 5 s on background and 15 s on peak. For crystals, the beam size was 1 μm with a counting time of 20 and 10 s on peaks and background, respectively. The following standards have been adopted for the various chemical elements: jadeite (Si and Na), corundum (Al), forsterite (Mg), andradite (Fe), rutile (Ti), orthoclase (K), barite (Ba), apatite (P), spessartine (Mn) and chromite (Cr). Sodium and potassium were analyzed first to reduce possible volatilization effects. Precision was better than 5% for all cations.

4. RESULTS

4.1 Clinopyroxene component calculation

Clinopyroxene components discussed in this study were calculated using procedures reported in Putirka et al. (1996) and modified in Putirka (1999). Molecular components were calculated on the basis of six oxygen atoms. The charge balance equation of Lindsley (1980) was applied to all the analyses for a nominal determination of Fe^{3+}. The Al^{IV} is taken as 2 – Si, with the remaining Al assigned to the M1 octahedral site. Fe^{3+} is then recalculated as follows: $Al^{VI} + {}^{M1}Fe^{3+} + {}^{M1}Cr + 2\ {}^{M1}Ti^{4+} = Al^{IV} + {}^{M2}Na$. We must warn, however, that while this equation can be useful to assess gross inconsistencies in EPMA analyses of pyroxenes, Mossbauer spectroscopic analyses of crystals (e.g., McGuire et al. 1989) show that such calculated Fe^{3+} contents have no correlation to measured Fe^{3+} contents. Without Mossbauer data, there is only one useful course of action, which is to assume that all Fe in pyroxene is as

Fe^{2+} provided that: 1) the range of experimental fO_2 conditions match those of the natural samples to which the models are applied (as it is the case of this study), and 2) natural samples are treated in the same was as experimental calibration data. The jadeite (Jd; $NaAlSi_2O_6$) component is assumed equal to the amount of Na or octahedral Al ($Al^{VI} = Al^{tot} - Al^{IV}$; $Al^{IV} = 2 - Si$), whichever is less. The CrCa-Tschermak component (CrCaTs; $CaCr_2SiO_6$ = Cr/2) is then calculated. The Ca-Tschermak (CaTs; $CaAl^{VI}Al^{IV}SiO_6$) component is equal to any remaining Al^{VI} (CaTs = Al^{VI} - Jd). Al^{IV} in excess is used to form CaTi-Tschermak [CaTiTs; $CaTiAl_2O_6 = (Al^{IV} – CaTs)/2$] and CaFe-Tschermak (CaFeTs; $CaFeSiAlO_6$) components. Only Fe^{2+} and Mg are used for calculation of the enstatite (En; $Mg_2Si_2O_6$) and ferrosilite (Fs; $Fe_2Si_2O_6$). Total iron is chose to determine diopside (Di, $CaMgSi_2O_6$) and hedenbergite (Hd; $CaFeSi_2O_6$) components. All calcium remaining after forming Ts, i.e. the sum of CaTs, CaFeTs, CrCaTs and CaTiTs, gives DiHd (DiHd = Ca – Ts). The enstatite-ferrosilite (EnFs) component is equal to one-half the FeO+MgO component remaining after forming DiHd [EnFs = (FeO+MgO - DiHd)/2]. At the equilibrium condition, clinopyroxene components calculated by this scheme should be very close to unity (see also Putirka et al. 1996; Putirka 1999).

4.2 Clinopyroxene compositional variations

Clinopyroxene analyses from our experiments are reported in Table 1SD provided as supplementary data. Each major cation incorporated in the crystals varies systematically as a function of cooling rate (Fig. 1a). From low (and isothermal condition) to high cooling rates, average clinopyroxene analyses are progressively depleted in Ca and Mg counter balanced by enrichments in Na, Al (mainly Al^{IV}), and Ti (Fig. 1a and Table 1SD). The contents of Di and Hd are both observed to decrease with increasing cooling rate (Fig. 1b and Table 1SD); the opposite occurs for the amounts of Fs, Jd and Ts, as the clinopyroxenes similarly freeze in

progressively higher temperatures, as cooling rate is increased. Thus, during cooling, Di and Hd components are consumed in favour of Ts, Jd, En and Fs (cf. Mollo et al. 2010) as follows:

$$(\text{Di-Hd})_{ss}^{cpx} + \text{melt} \rightarrow (\text{Ts-Jd-En-Fs})_{ss}^{cpx} \quad (1)$$

As the degree of cooling is increased, clinopyroxenes are characterized by the substitution of $^{M2}(Mg, Fe^{2+})$ with $^{M1}(Al, Fe^{3+})$ coupled with the substitution of ^{T}Si with ^{T}Al to form the CaTs component (Etzel et al. 2007). Notably, the progressive CaFeTs molecular increment compensates the decrement of ^{M1}Al with $^{M1}Fe^{3+}$. In this view, highly charged cations, such as Ti^{+4} and Fe^{3+} (Fig. 1a and Table 1SD), are accommodated in the M1 site of clinopyroxene due to the exchange reaction required to balance the charge deficiency caused by the substitution of Al for Si in the tetrahedral site (cf. Hill et al. 2000).

5. DISCUSSION

5.1 A new test for equilibrium

Putirka (2008) has recently observed that, in the case of clinopyroxene, the Fe-Mg exchange coefficient derived from 1,245 experimental observations yields $^{cpx\text{-}melt}Kd_{Fe\text{-}Mg}$ = 0.28±0.08 that is slightly higher than the range (0.27±0.03) previously considered (e.g., Putirka et al. 2003). However, the Fe-Mg exchange coefficient is not perfectly invariant and, consequently, accounts for a slightly temperature dependency that can be modeled (cf. Putirka 2008). Using the T-sensitive model for $^{cpx\text{-}melt}Kd_{Fe\text{-}Mg}$ derived by Putirka (2008) (see the spreadsheet available on line as supplementary material), we examine the partitioning of Mg and Fe between clinopyroxenes and melts from our experiments (Fig. 2). Results yield a fairly close correspondence (0.27±0.01) to the equilibrium range of 0.27±0.03 by Putirka et al.

(2003) and 0.28±0.08 by Putirka (2008) irrespective of whether the clinopyroxenes grew at isothermal equilibrium experimental conditions, or conditions of forced disequilibrium, i.e., under a constant cooling rate (Fig. 2). A similar equilibrium range ($^{cpx\text{-}melt}Kd_{Fe\text{-}Mg}$ = 0.27±0.02) is also obtained when we attempt to use the charge balance equation of Lindsley (1980) and the algorithm of Kress and Carmichael (1991) to calculate Fe^{2+} in clinopyroxene and melt, respectively.

The constancy of $^{cpx\text{-}melt}Kd_{Fe\text{-}Mg}$ under disequilibrium conditions has remarkable implications in the use of thermometers based on clinopyroxene compositions. Indeed, it is never possible to guarantee that a given clinopyroxene-melt pair is at equilibrium, and so can be used to estimate temperature. However, in an early study, Putirka (1999) proposed a model to test the equilibrium for clinopyroxene-bearing rocks. The model is based on the deviation of clinopyroxene components, i.e. Di, Hd, En, Fs, CaTs, CaTiTs, CaCrTs and Jd, between crystal and melt from equilibrium values. The degree of disequilibrium is determined through the comparison between components "predicted" for clinopyroxene via regression analyses of clinopyroxene-liquid pairs in equilibrium conditions, with those "measured" in the analyzed crystals. Using this model, Putirka (2008) and Mollo et al. (2010) suggested that the difference between "predicted" and "observed" components provide a more robust test for equilibrium than $^{cpx\text{-}melt}Kd_{Fe\text{-}Mg}$.

We present an improvement of the model of Putirka (1999) based on new global regression analyses performed by means of a broad experimental data set from LEPR (Library of Experimental Phase Relations; http://lepr.ofm-research.org). Anhydrous data were used for the regression analysis, whereas hydrous compositions were used as a "test data" to calculate the error associated with the estimate (cf. Putirka 2008). New global regressions offer no improvement in the prediction of CaTs, CaTiTs, CaCrTs and Jd components. We infer that data from literature concerning the concentration of Al, Ti, Cr and Na in clinopyroxene and

melt may be affected by large analytical errors, hampering an improvement of the model based on CaTs, CaTiTs, CaCrTs and Jd components. Alternatively, the analyses may be correct, but the measurements do not carefully compare melts adjacent to the crystal rims (cf. Putirka 2008) introducing a systematic error in the regression analysis. For the same set of compositions, the following equations are identical to those in Putirka (1999):

$$\ln\left(X_{CaTs}^{cpx}\right) = 2.58 + 0.12\frac{P(kbar)}{T(K)} - 9\times10^{-7}\frac{P^2(kbar)}{T(K)} + 0.78\ln\left[X_{Ca}^{liq}\left(X_{Al}^{liq}\right)^2 X_{Si}^{liq}\right] - 4.3\times10^3\frac{\left(X_{DiHd}^{cpx}\right)^2}{T(K)}$$

(R^2 = 0.77 and SEE = 0.03)

(2)

$$\ln\left(X_{CaTiTs}^{cpx}\right) = 5.1 + 0.52\ln\left[X_{Ca}^{liq}\left(X_{Al}^{liq}\right)^2 X_{Ti}^{liq}\right] + 2.04\times10^3\frac{\left(X_{DiHd}^{cpx}\right)^2}{T(K)} - 6.2X_{Si}^{liq} + 42.5X_{NaAl}^{liq} - 45.1X_{FeMgAl}^{liq}$$

(R^2 = 0.60 and SEE = 0.01)

(3)

$$\ln\left(\frac{X_{CaCrTs}^{cpx}}{X_{Ca}^{liq}\left(X_{Cr}^{liq}\right)^2 X_{Si}^{liq}}\right) = 12.8 \pm 1.8$$

(R^2 = 0.61 and SEE = 0.01)

(4)

$$\ln\left(X_{Jd}^{cpx}\right) = -1.06 + 0.13\frac{P(kbar)}{T(K)} - 6\times10^{-7}\frac{P^2(kbar)}{T(K)} + 1.02\ln\left[X_{Na}^{liq}X_{Al}^{liq}(X_{Si}^{liq})^2\right] - 0.80\ln(X_{Al}^{liq}) - 2.2\ln(X_{Si}^{liq})$$

(R^2 = 0.81 and SEE = 0.02)

(5)

By contrast, new regression analyses of EnFs (i.e. enstatite + ferrosilite) and DiHd (i.e. diopside + hedenbergite) produce improved fits according to the following equations:

$$\ln\left(X_{EnFs}^{cpx}\right) = 0.018 - 9.61X_{CaO}^{liq} + 7.46X_{MgO}^{liq}X_{SiO_2}^{liq} - 0.34\ln\left(X_{AlO_{1.5}}^{liq}\right) - 3.78\left(X_{NaO_{0.5}}^{liq} + X_{KO_{0.5}}^{liq}\right) - 3737.3\frac{\left(X_{DiHd}^{cpx}\right)^2}{T(K)} - 46.8\frac{P(kbar)}{T(K)}$$

(R^2 = 0.93 and SEE = 0.05)

(6)

$$\ln\left(X_{DiHd}^{cpx}\right) = -2.18 - 3.16X_{TiO_2}^{liq} - 0.365\ln\left(X_{AlO_{1.5}}^{liq}\right) + 0.05\ln\left(X_{MgO}^{liq}\right) - 3858.2\frac{\left(X_{EnFs}^{cpx}\right)^2}{T(K)} + \frac{2107.4}{T(K)} - 17.64\frac{P(kbar)}{T(K)}$$

(R^2 = 0.92 and SEE = 0.06)

(7)

Regression analyses plotted in Fig. 3 indicate that these new models are highly correlated with deviations in observed and calculated values for both EnFs and DiHd. To test Equations (6) and (7) we have used as input data clinopyroxene-melt pairs from (i) our

anhydrous cooling rate experiments and (ii) hydrous equilibrium experiments by Metrich and Rutherford (1999) conducted on a similar Etnean trachybasalt equilibrated at 27-80 MPa and 1135–1009 °C with a melt-water content of 1.3-3.1 wt.%. All these compositions are reported in a downloadable spreadsheet available online as supplementary material and were not included into the calibration dataset of Equations (6) and (7), offering an independent test for our models. Results from computations are plotted in Fig. 4, showing that variations between "observed" and "predicted" clinopyroxene components are generally measured for DiHd due to the abundance of Di and Hd into clinopyroxene crystals. However, as the degree of cooling is increased, data from our experiments progressively depart from the equilibrium line (Fig. 4). This deviation mainly occurs in response to the kinetically-controlled exchange reaction (1), as Di and Hd are consumed to form Ts (Fig. 1). In contrast, equilibrium data from Metrich and Rutherford (1999) and this study closely approach to the equilibrium line, demonstrating the reliability of our new test for equilibrium under hydrous and anhydrous crystallization conditions of Etnean magmas.

5.2 Thermometry

We have used clinopyroxene-melt pairs from our experiments as input data for thermometric Equation (33) [hereafter referred to as Equation (8)] of Putirka (2008) whose activity model is:

$$Eqn.33 = \frac{10^4}{T(K)} = 7.53 - 0.14\ln\left(\frac{X_{Jd}^{cpx} X_{CaO}^{liq} X_{FeMg}^{liq}}{X_{DiHd}^{cpx} X_{Na}^{liq} X_{Al}^{liq}}\right) + 0.07\left(H_2O^{liq}\right) - 14.9\left(X_{CaO}^{liq} X_{SiO_2}^{liq}\right) - 0.08\ln\left(X_{TiO_2}^{liq}\right) - 3.62\left(X_{NaO_{0.5}}^{liq} + X_{KO_{0.5}}^{liq}\right) - 1.1\left(Mg\#^{liq}\right) - 0.18\ln\left(X_{EnFs}^{cpx}\right) - 0.027P(kbar)$$

(8)

Equation (8) is based on the Jd-DiHd exchange reaction (Putirka et al. 1996, 2003) and has a low uncertainty (40 °C) due to new global calibrations including a greater number of compositions obtained at pressures lower than 7 GPa (Putirka 2008). In Fig. 5 the temperature estimates obtained by Equation (8) are plotted as a function of experimental conditions. At the equilibrium condition, the predicted temperature matches with the experimental temperature of 1100 °C. However, the temperature estimates increase systematically as the cooling rate is increased, depicting monotonic trends towards overestimates of temperature relative to the final temperature before rapid quenching (Fig 5). At the fastest cooling rate of 50 °C/h, the predicted temperatures approach the liquidus temperature, suggesting that early-formed crystals do not re-equilibrate with the melt. Therefore, in the case of rapidly cooled clinopyroxene-melt pairs, lower crystallization temperatures might not be revealed by the use of thermometric Equation (8), unless new crystals nucleate or the system approaches to the equilibrium. In other words, the thermometer would predict crystallization temperatures somewhere between the saturation temperature of clinopyroxene, and the final resting temperature of the system, i.e. the closure temperature of crystal-growth kinetics at the time of quenching (Fig. 5). For example, in naturally solidifying melts, the rapid growth of clinopyroxene can be halted by variations in thermal conditions or by the crystallization of a new phase. Indeed, at Mt. Etna volcano, it has been demonstrated that the growth of clinopyroxene is hindered by the crystallization of plagioclase (Armienti et al. 1984, 1994).

To decipher the thermal path of clinopyroxene-bearing rocks, the difference (ΔDiHd expressed as absolute value) between the "predicted" and "observed" components of DiHd calculated by Equation (7) has been plotted *versus* the difference (ΔT) between the clinopyroxene crystallization temperature predicted by Equation (8) and the resting temperature of the system (Fig. 6). This plot highlights that the thermal pathway (i.e., ΔT) is positively correlated with the deviation from equilibrium condition of the clinopyroxene (i.e.,

ΔDiHd). The regression analysis of the data yields the following equation:

$$\Delta T(^{\circ}C) = -20.87 + 650.39\Delta DiHd \quad (9)$$

In Fig. 7, ΔT values "predicted" by Equation (9) are plotted *versus* those "observed" from our cooling rate experiments yielding low uncertainties for our calibration data (R^2 = 0.96 and SEE = 9.88). Within the thermal path estimated by Equation (9), clinopyroxene crystals grow over an ever-changing temperature whose range is bounded by the liquidus and the final solidification temperature of the system. Under dynamic crystallization conditions, indeed, there is no single equilibrium temperature, but a range of relevant temperatures in which the crystals attempt to re-equilibrate with the melt. Since variable thermal regimes influence the solidification path of melts at post-eruptive conditions, Equation (9) can be used to estimate the temperature range of clinopyroxene-bearing lava flows and dikes at Mt. Etna volcano.

5.3 The limits of Equations (9)

To test Equation (9), we have used clinopyroxene-melt pairs reported in cooling rate studies by Conte et al. (2006), Hammer (2006) and Mollo et al. (2012) which are external to the calibration dataset (see the spreadsheet available on line as supplementary material). As in the case of our cooling rate data (Fig. 4), each cooling rate used in each laboratory caused departures from equilibrium and, consequently, a variety of ΔT values. In particular, cooling rate experiments by Conte et al. (2006) were conducted on a trachybasalt, an andesitic basalt and a basaltic andesite, taken as representative of shoshonite, high-K-calcalkaline and calcalkaline compositions. Conversely, dynamic crystallization experiments by Mollo et al.

(2012) and Hammer (2006) were carried out using as starting materials a basaltic andesite and an Fe-rich tholeiitic basalt, respectively. Results from calculations are displayed in Fig. 8, which shows that Equation (9) fails for a large number of data from cooling rate experiments by Conte et al. (2006) and Mollo et al. (2012). Much higher uncertainties are, however, measured for rapidly cooled clinopyroxene-melt pairs by Hammer (2006). Generally, Equation (9) fails as the FeO_{tot}/Al_2O_3 ratio of clinopyroxene increases (Fig. 8). This suggests that the model should be used with predominantly Etnean alkaline magmas and so we caution against the application of our model to compositions that fall outside of the range of compositions included into the calibration dataset.

5.4 The thermal path of Etnean lava flows and dikes

In order to highlight the implications of Equation (9) for deciphering the solidification path of melts at post-eruptive conditions, we have used as input data clinopyroxene-melt pairs from naturally cooled Etnean lava flow and dike samples reported by Tanguy et al. (1997) and Mollo et al. (2011b), respectively. These data are included in the spreadsheet available on line as supplementary material. We highlight that $^{cpx\text{-}melt}Kd_{Fe\text{-}Mg}$ determined by the T-sensitive model of Putirka (2008) ranges from 0.24 to 0.27, suggesting equilibrium crystallization of clinopyroxene microphenocrysts from lava flow and dike samples. In contrast, $\Delta DiHd$ calculated by Equation (7) shows significant variations from 0.01 to 0.16, indicating strong disequilibrium conditions for some naturally cooled clinopyroxene-melt pairs (see the spreadsheet available on line as supplementary material).

For each crystallization temperature predicted by the thermometric Equation (8), we have determined ΔT using Equation (9). Results are plotted in Fig. 9 showing that ΔT values of lava flows vary from 0.03 to 80.72 °C. Although lava flows solidified under variable thermal regimes, the thermometric Equation (8) predicts one single crystallization

temperature somewhere between the saturation temperature of clinopyroxene and the final solidification temperature of the system. Only four lava samples show ΔT values lower than the uncertainty (10 °C) of Equation (9) suggesting equilibrium crystallization (Fig. 9). In addition to the analysis of clinopyroxene in lava flows, Tanguy et al. (1997) have sometimes reported the chemistry of co-existing titanomagnetites. Using these crystal compositions as input data for a geospeedometry model based on Ti-Al-Mg redistribution in titanomagnetite, Mollo et al. (2013b) have calculated the cooling rate conditions of Etnean lava flows. These results are reported in Fig. 9 demonstrating that ΔT increases as the cooling rate is increased, in agreement with the experimental trend showed in Fig. 5. The same positive correlation is also observed for clinopyroxene-melt pairs analyzed from innermost to the outermost portion of a dike outcropping at Mt. Etna volcano (Fig. 9). By means of thermal models, Mollo et al. (2011b) measured faster cooling rates (0.96-79.8 °C/h) from dike core-to-rim that match with the increasing ΔT values (6.13-29.37 °C) predicted through Equation (9) (Fig. 9).

6. CONCLUSIONS

When clinopyroxenes nucleate and grow in response to dynamic crystallization conditions, their compositions do not have time enough to equilibrate with the melt. Thus, the use of rapidly cooled clinopyroxene-melt pairs as input data for thermometric models indicates that clinopyroxenes record successively higher temperatures as the rate of cooling is increased. The best test for assessing whether or not clinopyroxene crystals and co-existing melts were in equilibrium at the time of crystallization is the comparison between “predicted” and “observed” components in clinopyroxene. The variation of DiHd component is positively correlated with the difference between the clinopyroxene saturation temperature predicted by the thermometer and the final temperature of crystal-growth kinetics. Modeling this relationship, we can determine the clinopyroxene-melt pairs more suitable to estimate the

equilibrium crystallization condition of Etnean melts as well as the solidification path of clinopyroxene microphenocrysts at post-eruption conditions.

ACKNOWLEDGEMENTS

Authors are grateful to G. Iezzi and D. B. Dingwell for their constructive comments. A. Cavallo is acknowledged for assistance during electron microprobe analysis. S. Mollo was supported by the ERC Starting grant 259256 GLASS project.

REFERENCES

Armienti, P., Barberi, F., Innocenti, F., Pompilio, M., Romano, R., Villari, L., 1984. Compositional variation in the 1983 and other recent Etnean lavas: insights on the shallow feeding system. Bull. Volcanol. 47, 995-1007.

Armienti, P., Pareschi, M.T., Pompilio, M., Innocenti, F., 1994. Effects of magma storage and ascent on the kinetics of crystal growth: the case of the 1991-1993 Mt. Etna eruption. Contr. Mineral. Petrol. 115, 402-414.

Armienti, P., Perinelli, P., Putirka, K., 2012. A New Model to Estimate Deep-level Magma Ascent Rates, with Applications to Mt. Etna (Sicily, Italy). J. Petrol. doi: 10.1093/petrology/egs085.

Baginski, B., Dzierzanowski, P., Macdonald, R., Upton, B.G.J., 2009. Complex relationships among coexisting pyroxenes: the Paleogene Eskdalemuir dyke, Scotland. Mineral. Mag. 73, 929-942.

Baker M.B., Grove T.L., 1985. Kinetic controls on pyroxene nucleation and metastable liquid lines of descent in a basaltic andesite. Am. Mineral. 70, 279–287.

Bonaccorso, A., Currenti, G., Del Negro C., Boschi E., 2010. Dike deflection modelling for inferring magma pressure and withdrawal, with application to Etna 2001 case. EPSL

293, 121–129.

Cashman, K.V., 1993. Relationship between plagioclase crystallization and cooling rate in basaltic melts. Contr. Mineral. Petrol. 113**,** 126–142.

Coish, R.A., Taylor, L.A., 1979. The effect of cooling rate on texture and pyroxene chemistry in DSDP Leg 34 basalt: A microprobe study. EPSL 42, 389-398.

Conte, A.M., Perinelli, C., Trigila, R., 2006. Cooling kinetics experiments on different Stromboli lavas: effects on crystal morphologies and phases compositions. J. Vol. Geotherm. Res. 155, 179-200.

Corsaro, R.A., Civetta, L., Di Renzo, V., Miraglia, L., 2009. Petrology of lavas from the 2004–2005 flank eruption of Mt. Etna, Italy: inferences on the dynamics of magma in the shallow plumbing system. Bull. Vol. 71, 781–793.

Corsaro R.A., Cristofolini R., Patanè L., 1996. The 1669 eruption at Mount Etna: Chronology, petrology and geochemistry, with inference on magma sources and ascent mechanisms. Bull. Vol. 58, 348-358.

Del Gaudio, P., Mollo, S., Ventura, G., Iezzi, G., Taddeucci, J., Cavallo, A., 2010. Cooling rate-induced differentiation in anhydrous and hydrous basalts at 500 MPa: Implications for the storage and transport of magmas in dikes. Chem. Geol. 270, 164-178.

Etzel, K., Benisek, A., Dachs, E., Cemic, L., 2007. Thermodynamic mixing behavior of synthetic Ca-Tschermak–diopside pyroxene solid solutions: I. Volume and heat capacity of mixing. Phys. Chem .Minerals 34, 733–746.

Faraone, D., Molin, G., Zanazzi, P.F., 1988. Clinopyroxene from Vulcano (Aeolian Islands, Italy): Crystal chemistry and cooling history. Lithos 22, 113-126.

Gamble, R.P., Taylor, L.A., 1980. Crystal/liquid partitioning in augite: Effects of cooling rate. EPSL 47, 21-33.

Gee L. L., Sack R. O., 1988. Experimental petrology of melilite nephelinites. J. Petrol. 29,

1235–1255.

Gottsmann, J., Harris, A.J.L., Dingwell, D.B., 2004. Thermal history of Hawaiian pahoehoe lava crusts at the glass transition: implications for flow rheology and emplacement. EPSL 228, 343-353.

Grove, T.L., Bence, A.E., 1977. Experimental study of pyroxene-liquid interaction in quartz-normative basalt 15597. Proceedings of Lunar and Planetary Science Conference, 8th, 1549-1579.

Grove, T.L., Bence, A.E., 1979. Crystallization kinetics in a multiply saturated basalt magma: An experimental study of Luna 24 ferrobasalt. Proceedings of Lunar and Planetary Science Conference**,** 10th, 439-478.

Grove, T.L., Bryan, W.B., 1983. Fractionation of pyroxene-phyric MORB at low pressure: an experimental study. Contr. Mineral. Petrol. 84, 293-309.

Grove, T.L., Raudsepp, M., 1978. Effects of kinetics on the crystallization of quartz-normative basalt 15597: An experimental study. Proceedings of Lunar and Planetary Science Conference**,** 9th, 585-599.

Hammer, J.E., 2006. Influence of fO_2 and cooling rate on the kinetics and energetics of Fe-rich basalt crystallization. EPSL 248, 618-637.

Hammer, J.E., 2008. Experimental studies of the kinetics and energetics of magma crystallization. In: Putirka, K.D., Tepley, F.J. (Eds.), Minerals, Inclusions and Volcanic Processes: Reviews in Mineralogy and Geochemistry, 69, pp. 9-59.

Heap, M.J., Mollo, S., Vinciguerra, S., Lavallée, Y., Hess, K.-U., Dingwell, D.B., Baud P., Iezzi G., 2013. Thermal weakening of the carbonate basement under Mt. Etna volcano (Italy): Implications for volcano instability, J. Vol. Geother. Res. http://dx.doi.org/10.1016/j.jvolgeores.2012.10.004.

Hill, E., Wood, B.J., Blundy, J.D., 2000. The effect of Ca-Tschermaks component on trace

element partitioning between clinopyroxene and silicate melt. Lithos, 53, 203–215.

Kress, V.C., Carmichael, I.S.E., 1991. The compressibility of silicate liquids containing Fe_2O_3 and the effect of composition, temperature, oxygen fugacity and pressure on their redox states. Contr. Mineral. Petrol. 108, 82-92.

Lanzafame, G., Mollo, S., Iezzi, G., Ferlito, C., Ventura, G., 2013. Unravelling the solidification path of a pahoehoe "cicirara" lava from Mount Etna volcano. Bull. Vol., 75:703.

Latypov, R., Hanski, E., Lavrenchuk, A., Huhma, H., Havela T., 2011. A ”Three-Increase Model” for the Origin of the Marginal Reversal of the Koitelainen Layered Intrusion, Finland. J. Petrol. 52, 733-764.

Lindsley, D.H., 1980. Phase equilibria of pyroxenes at pressures >1 atmosphere. In: Prewitt C.T. (ed.), Pyroxenes (Reviews of Mineralogy vol. 7). Mineralogical Society of America, Washington DC, pp 289-308.

Lofgren, G.E., Huss, G.R., Wasserburg, G.J., 2006. An experimental study of trace-element partitioning between Ti-Al-clinopyroxene and melt: Equilibrium and kinetic effects including sector zoning. Am. Mineral. 91, 1596-1606.

Matzen, A. K., Baker, M. B., Beckett, J. R., Stolper E. M., 2011. Fe-Mg partitioning between olivine and high-magnesian melts and the nature of Hawaiian parental liquids. Journal of Petrology, 52, 1243-1263.

McGuire, A.V., Dyar, M.D., Ward, K.W., 1989. Neglected Fe^{3+}/Fe^{2+} ratios: A study of Fe^{3+} content of megacrysts from alkali basalts. Geology, 17, 687 -690

Metrich N., Clocchiatti C., 1989. Melt inclusion investigation of the volatile behaviour in historic alkali basaltic magmas of Etna. Bull. Vol. 51, 185-198.

Métrich, N., Rutherford, M.J., 1999. Low pressure crystallization paths of H_2O-saturated basaltic-hawaiitic melts from Mt Etna: Implications for open-system degassing of basaltic

volcanoes. Geochim. Cosmochim. Acta 62, 1195–1205.

Mevel, C., Velde, D., 1976. Clinopyroxenes in Mesozoic pillow lavas from the French Alps: influence of cooling rate on compositional trends. EPSL 32, 158–164.

Mollo, S., Del Gaudio, P., Ventura, G., Iezzi, G., Scarlato, P., 2010. Dependence of clinopyroxene composition on cooling rate in basaltic magmas: Implications for thermobarometry. Lithos, 118, 302-312.

Mollo S., Putirka K., Iezzi G., Del Gaudio P., Scarlato P., 2011a. Plagioclase-melt (dis)equilibrium due to cooling dynamics: implications for thermometry, barometry and hygrometry. Lithos**.** 125, 221-235.

Mollo S., Lanzafame G., Masotta M., Iezzi G., Ferlito C, Scarlato P., 2011b. Cooling history of a dike as revealed by mineral chemistry: A case study from Mt. Etna volcano. Chem. Geol. 288, 39-52, doi:10.1016/j.chemgeo.2011.06.016.

Mollo S., Vinciguerra S., Iezzi G., Iarocci A., Scarlato P., Heap M.J., Dingwell D.B., 2011c. Volcanic edifice weakening via devolatilization reactions. Geophys. J. Intern. 186, 1073-1077.

Mollo S., Misiti V., Scarlato P. Soligo M., 2012, The role of cooling rate in the origin of high temperature phases at the chilled margin of magmatic intrusions. Chem. Geol. 322-323, 28-46, doi:10.1016/j.chemgeo.2012.05.029.

Mollo, S., Scarlato, P., Lanzafame, G., Ferlito, C., 2013a. Deciphering lava flow post-eruption differentiation processes by means of geochemical and isotopic variations: A case study from Mt. Etna volcano, Lithos 162-163, 115-127, doi: 10.1016/j.lithos.2012.12.020.

Mollo, S., Putirka, K., Iezzi, G., Scarlato, P., 2013b. The control of cooling rate on titanomagnetite composition: Implications for a geospeedometry model applicable to alkaline rocks from Mt. Etna volcano. Contr. Mineral. Petrol. 165, 457-475, doi:

10.1007/s00410-012-0817-6.

Putirka, K., Johnson, M., Kinzler, R., Walker, D., 1996. Thermobarometry of mafic igneous rocks based on clinopyroxene-liquid equilibria, 0-30 kbar. Contr. Mineral. Petrol. 123, 92-108.

Putirka, K., 1999. Clinopyroxene + liquid equilibria. Contr. Mineral. Petrol. 135, 151-163.

Putirka, K., Ryerson, F.J., Mikaelian, H., 2003. New igneous thermobarometers for mafic and evolved lava compositions, based on clinopyroxene+liquid equilibria. Am. Mineral. 88, 1542-1554.

Putirka, K.D., 2008. Thermometers and barometers for volcanic systems. In: Putirka, K.D., Tepley, F. (Eds.), Minerals, Inclusions, and Volcanic Processes: Reviews in Mineralogy and Geochemistry, 69, pp. 61-120.

Roeder, P.L, Emslie, R.F., 1970. Olivine-liquid equilibrium. Contr. Mineral. Petrol.29, 275-289.

Sisson, T.W., Grove, T.L., 1993. Experimental investigations of the role of water in calc-alkaline differentiation and subduction zone magmatism. Contr. Mineral. Petrol. 113, 143-166.

Smith, D., Lindsley, D.H., 1971. Stable and metastable augite crystallization trends in a single basalt flow. Am. Mineral. 56, 225-233.

Tanguy, J.C., Condomines, M., Kieffer, G., 1997. Evolution of the Mount Etna magma: constraints on the present feeding system and eruptive mechanism. J. Vol. Geotherm. Res. 75, 221–250.

Tormey, D.R., Grove, T.L., Bryan, W.B., 1987. Experimental petrology of normal MORB near the Kane fracture zone: 22–25°N, mid-Atlantic ridge. Contr. Mineral. Petrol. 96, 121-139.

Ujike, O., 1982. Microprobe mineralogy of plagioclase, clinopyroxene and amphibole as

records of cooling rate in the Shirotori-Hiketa dike swarm, northeastern Shikoku, Japan. Lithos, 15, 281-293.

Viccaro, M., Ferlito, C., Cortesogno, L., Cristofolini, R., Gaggero, L., 2006. Magma mixing during the 2001 event at Mount Etna (Italy): effect on the eruptive dynamics. J. Vol. Geotherm. Res. 149, 139–159.

Wilding, M.C., Webb, S.L., Dingwell, D.B., 1995. Evaluation of a relaxation geospeedometer for volcanic glasses. Chem. Geol. 125, 137-148.

FIGURE CAPTIONS

Fig. 1. Variation of clinopyroxene cations (a) and components (b) as a function of experimental conditions. Di = diopside. Hd = hedenbergite. En = enstatite. Fs = ferrosilite. Jd = jadeite. Ts = Ca-Tschermak + CaFe-Tschermak + CaTi-Tschermak + CaCr-Tschermak. Data come from the average of core and rim analyses. At the scale of the figure, error bars are within the symbols.

Fig. 2. Variation of Fe-Mg element partitioning between clinopyroxene and melt (i.e., $^{cpx\text{-}melt}Kd_{Fe\text{-}Mg}$) as a function of experimental conditions. $^{cpx\text{-}melt}Kd_{Fe\text{-}Mg}$ has been obtained using the T-sensitive model proposed by Putirka (2008). All data agree with the equilibrium range of 0.27±0.03 (Putirka *et al.*, 2003) irrespective for equilibrium and disequilibrium experimental conditions.

Fig. 3. New global calibrations for EnFs (a) and DiHd (b) components performed by means of a broad experimental data set from LEPR (Library of Experimental Phase Relations; http://lepr.ofm-research.org). Anhydrous data were used for the regression analysis, whereas hydrous compositions were used as "test data" to calculate the error associated with the

estimate (cf. Putirka, 2008). These new models to test the equilibrium for clinopyroxene-bearing rocks are based on the deviation of clinopyroxene components, e.g. Di+Hd and En+Fs, between crystal and melt from equilibrium values. The degree of disequilibrium (Δ) is determined through the difference between components "predicted" for clinopyroxene via regression analyses of clinopyroxene-melt pairs in equilibrium conditions, with those "measured" in the analyzed crystals. R^2 = coefficient of determination. SEE = standard error of estimate. N = number of data points.

Fig. 4. To test new regression models from this study we have used data (i.e., clinopyroxene rim and co-existing melt) from our anhydrous cooling rate experiments conducted at atmospheric pressure and (ii) hydrous equilibrium experiments carried out on a similar trachybasalt from Mt. Etna (Metrich & Rutherford, 1999). All these compositions are reported in a downloadable spreadsheet available online as supplementary material. Our disequilibrium data progressively depart from the equilibrium line as a function of cooling rate, whereas compositions by Metrich & Rutherford (1999) closely approach to the equilibrium. DiHd = diopside + hedenbergite. EnFs = enstatite + ferrosilite. Ts = the sum of Ca-, CrCa-, CaTi-, CaFe-Tschermak components. Jd = jadeite. When the symbols are not observable, data overlap.

Fig. 5. Variation of the temperature estimate calculated by using clinopyroxene-melt pairs from our experiments as input data for Equation (8). The thermometer well predicts the equilibrium temperature of 1100 °C. In contrast, higher crystallization temperatures are progressively estimated with increasing cooling rate. When the symbols are not observable, data overlap.

Fig. 6. Regression analysis of data from this study. A linear fit is obtained for the thermal path of the system (ΔT) plotted *versus* the variation between "predicted" and "observed" diopside + hedenbergite (ΔDiHd) components in clinopyroxene. R^2 = coefficient of determination. SEE = standard error of estimate. N = number of data points. At the scale of the figure, error bars are within the symbols.

Fig. 7. Calibration of Equation (9) using data obtained at 0.1 MPa from this study. This new model allows to determine the thermal path (ΔT) experienced by clinopyroxene-melt pairs from alkaline rocks. R^2 = coefficient of determination. SEE = standard error of estimate. N = number of data points. At the scale of the figure, error bars are within the symbols.

Fig. 8. To test Equation (9) we have calculated the thermal path of the melt (ΔT) using clinopyroxene-melt pairs from previous cooling rate studies (Conte *et al.*, 2006; Hammer 2006; Mollo *et al.*, 2012). Results indicate that our test fails as the FeO_{tot}/Al_2O_3 ratio of clinopyroxene increases, accounting for iron enrichments and aluminium depletions during the transition from calcalkaline to tholeiitic compositions. The lowest uncertainty is obtained for alkaline rocks. At the scale of the figure, error bars are within the symbols.

Fig. 9. Clinopyroxene-melt pairs from naturally cooled lava flow and dike samples at Mt. Etna volcano are used as input data for Equation (9). The measured thermal ranges (ΔT) are compared with the clinopyroxene crystallization temperature predicted by the thermometric Equation (8). Values of ΔT lower than the uncertainty (SEE = 10) of Equation (9) suggest equilibrium crystallization. In contrast, increasing ΔT values are positively correlated with increasing cooling rate conditions measured for some lava flow and dike samples. The dotted circles indicate the lava samples reported by Tanguy *et al.* (1997) that was used to calculate

the cooling rate by means of a geospeedometer based on Ti-Mg-Al redistribution in titanomagnetite.

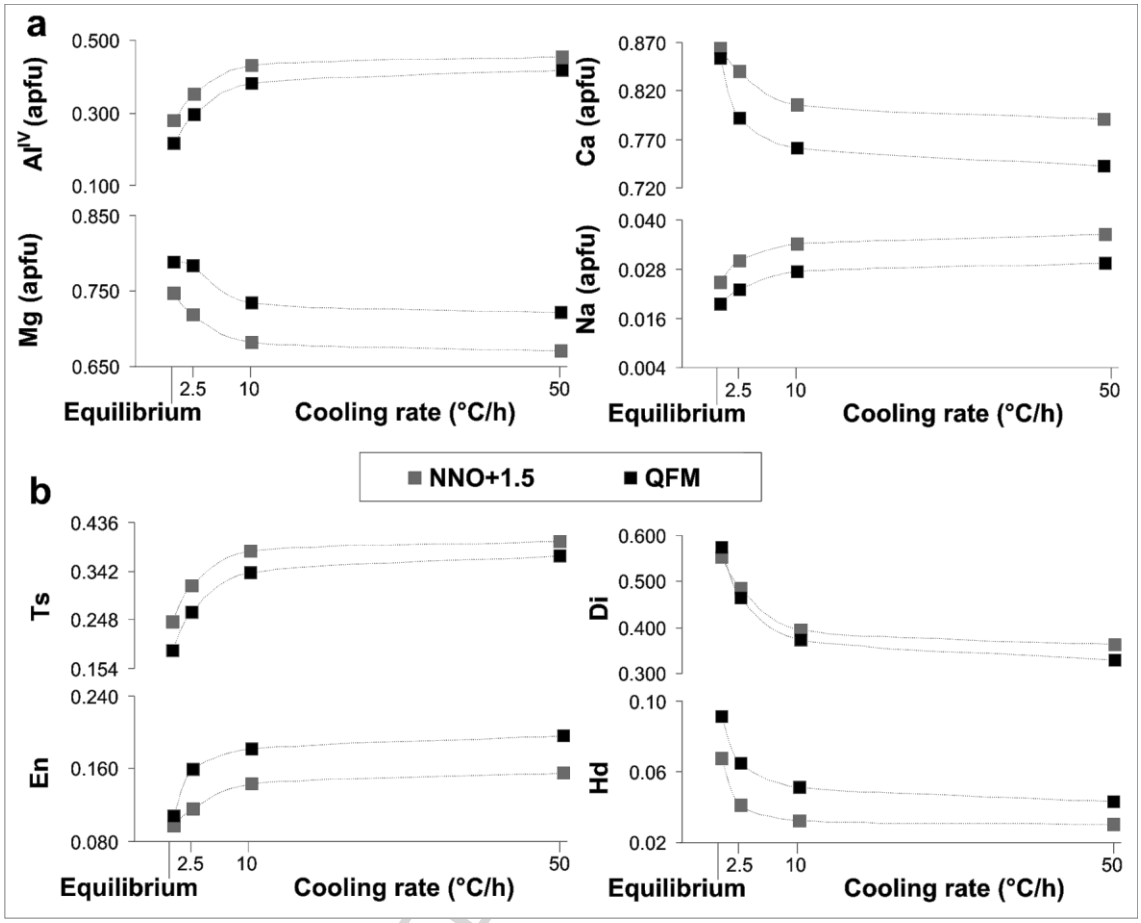

Fig. 1

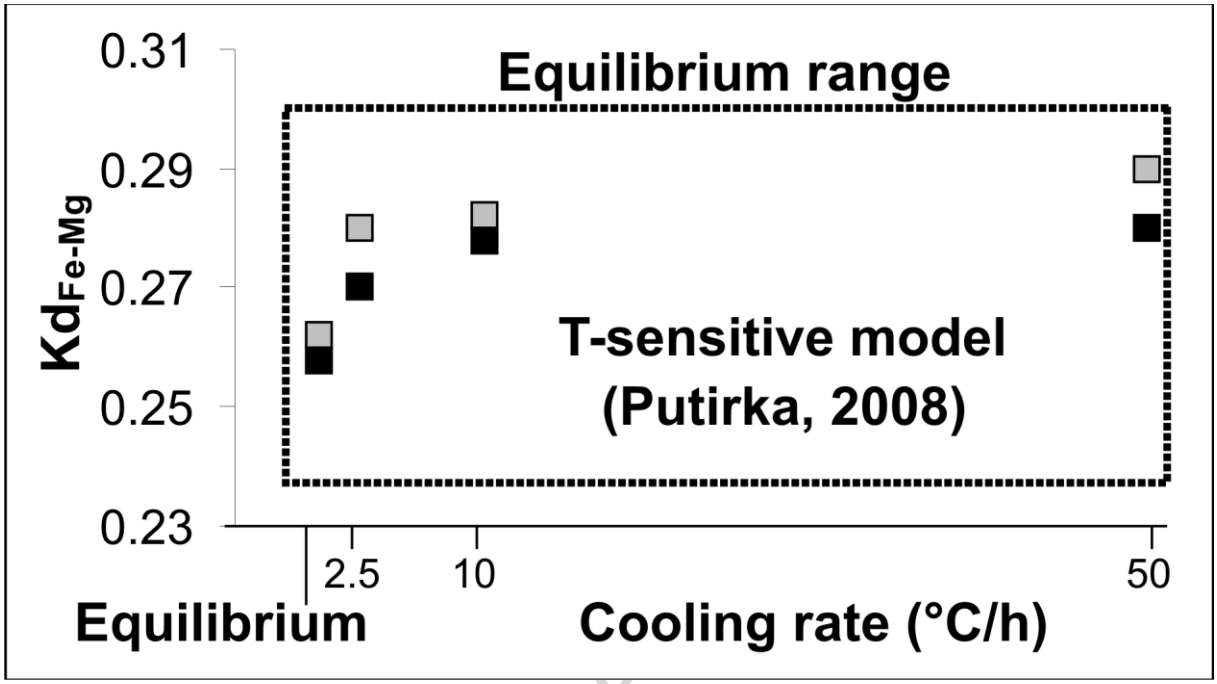

Fig. 2

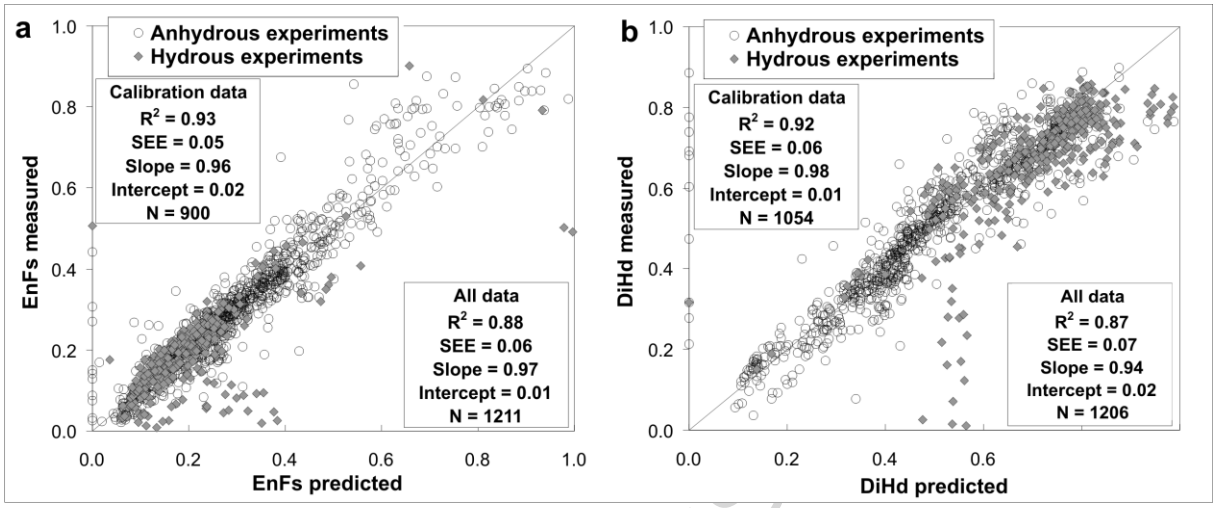

Fig. 3

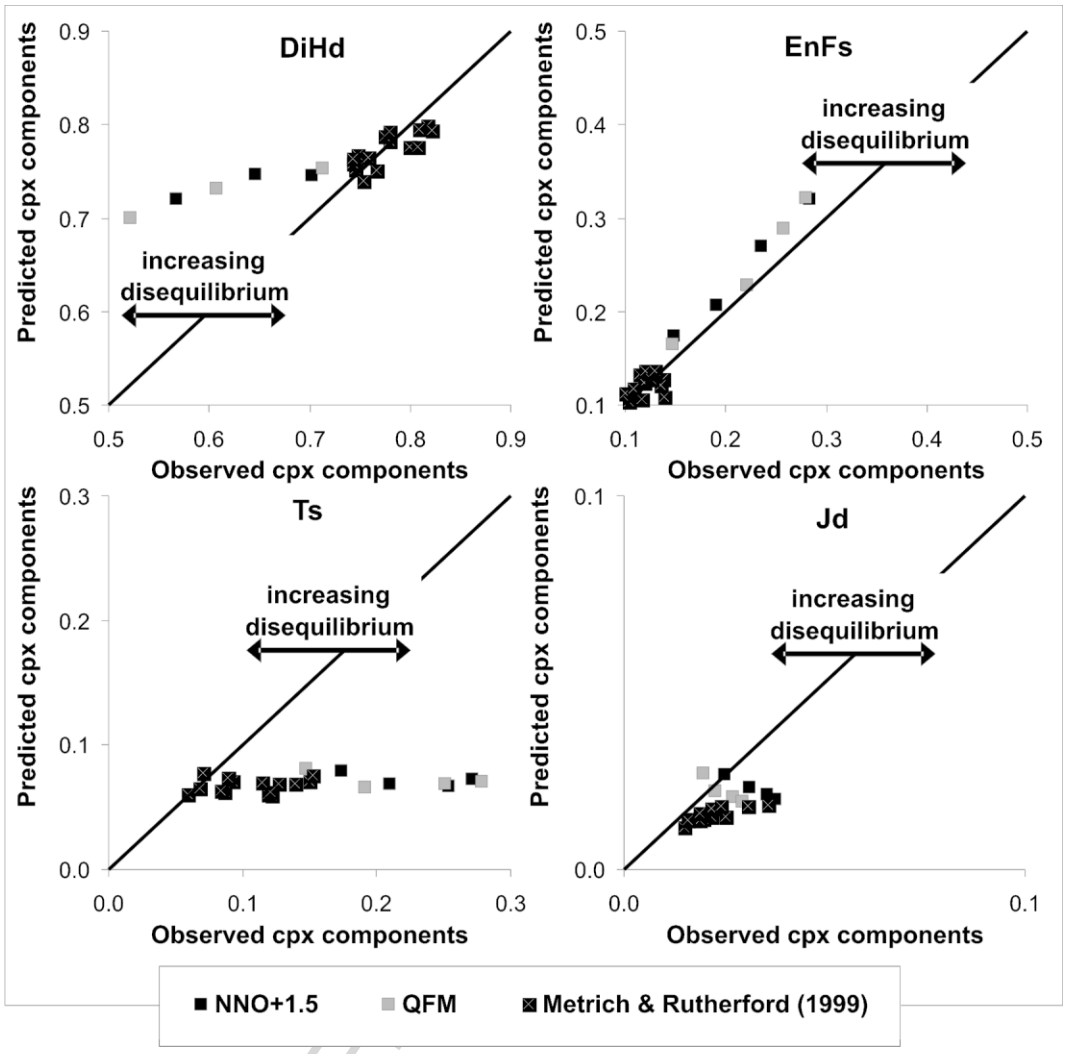

Fig. 4

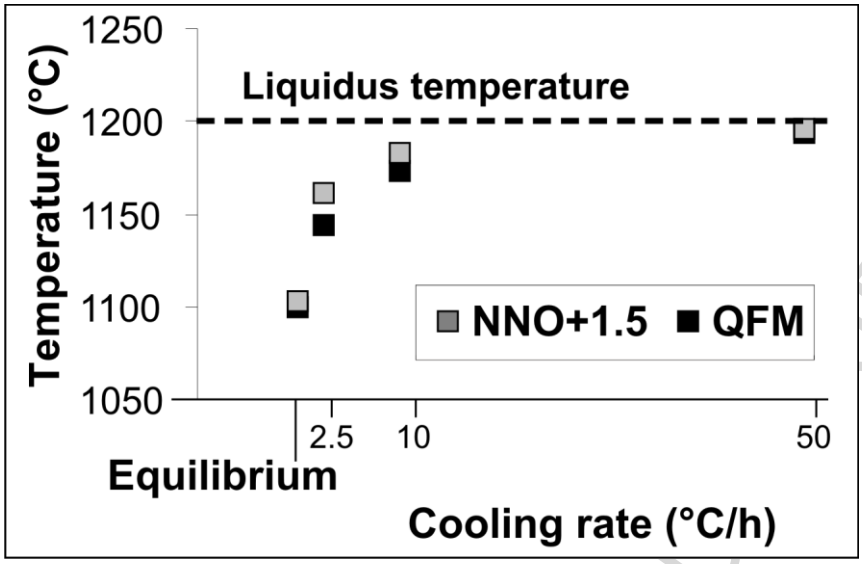

Fig. 5

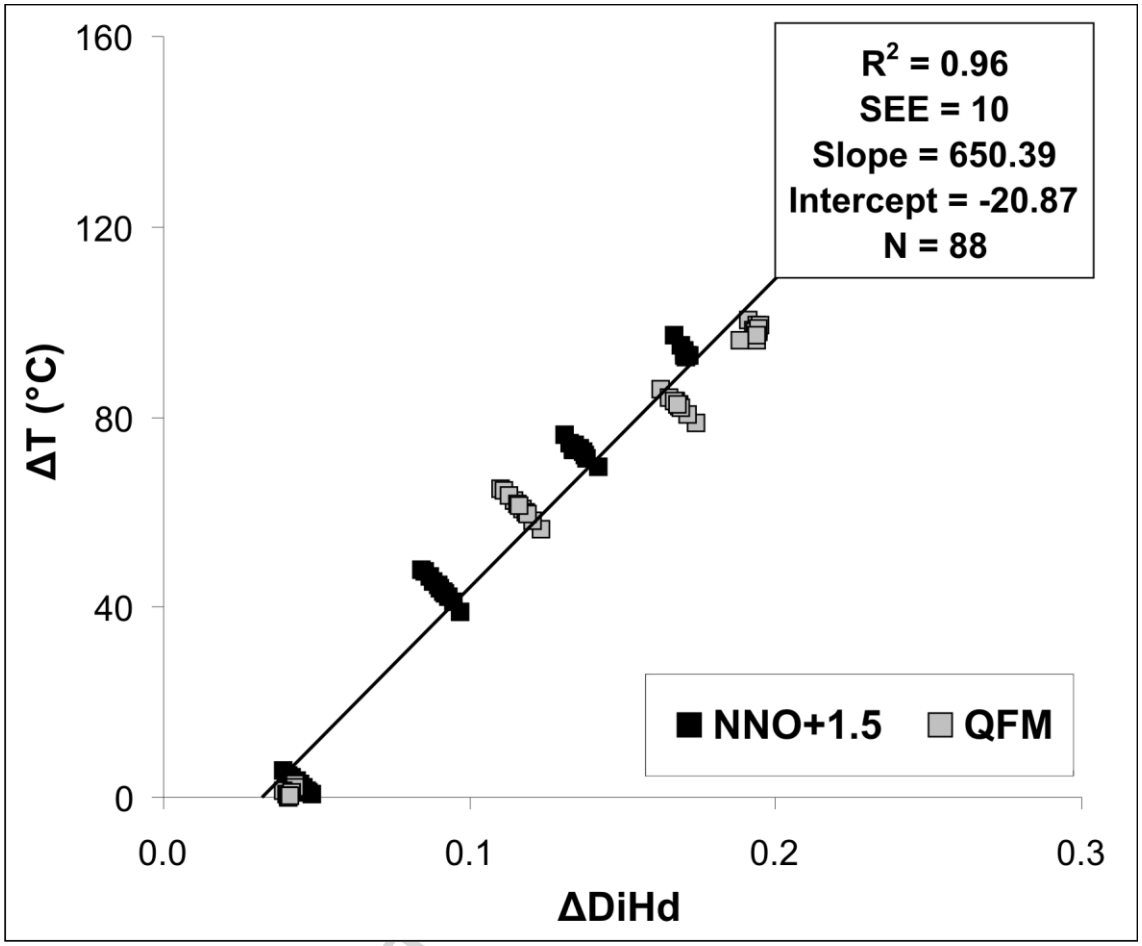

Fig. 6

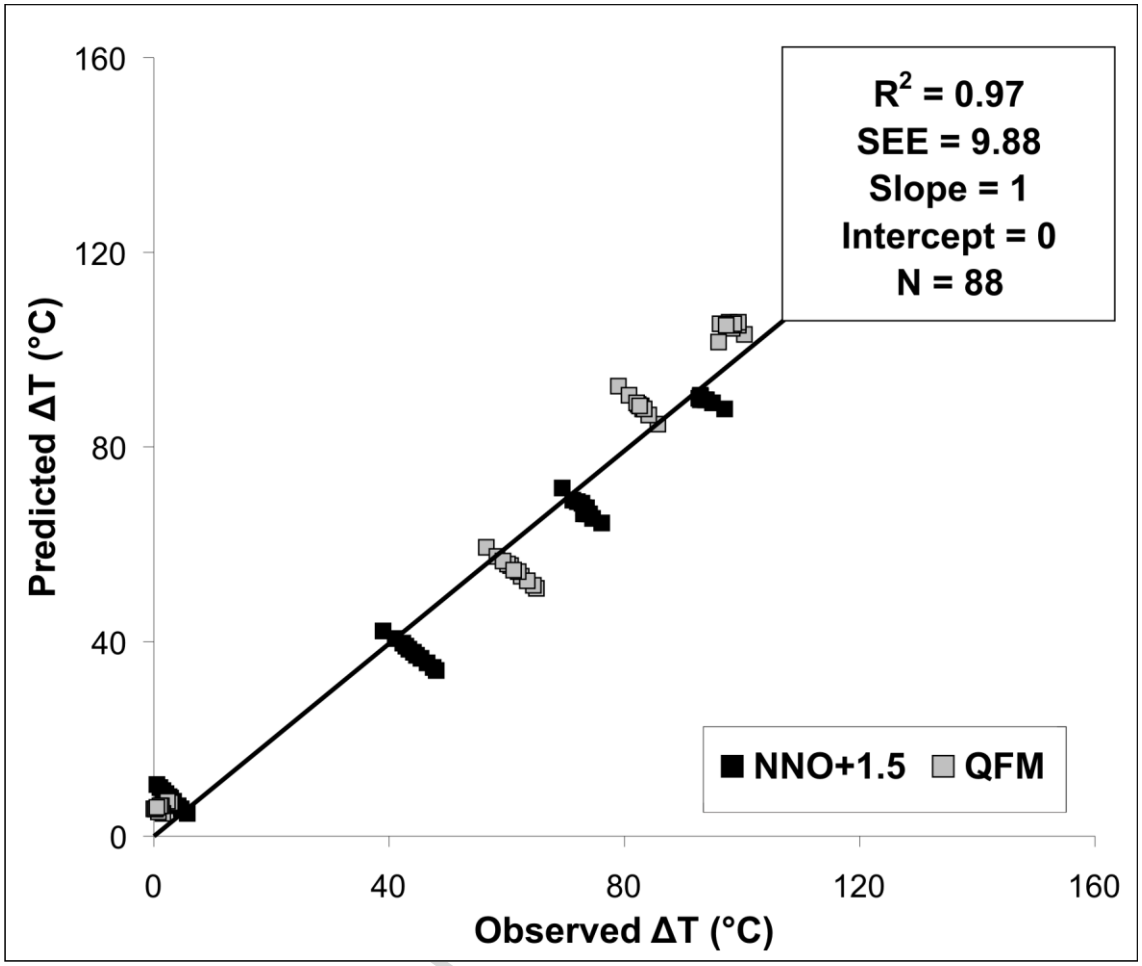

Fig. 7

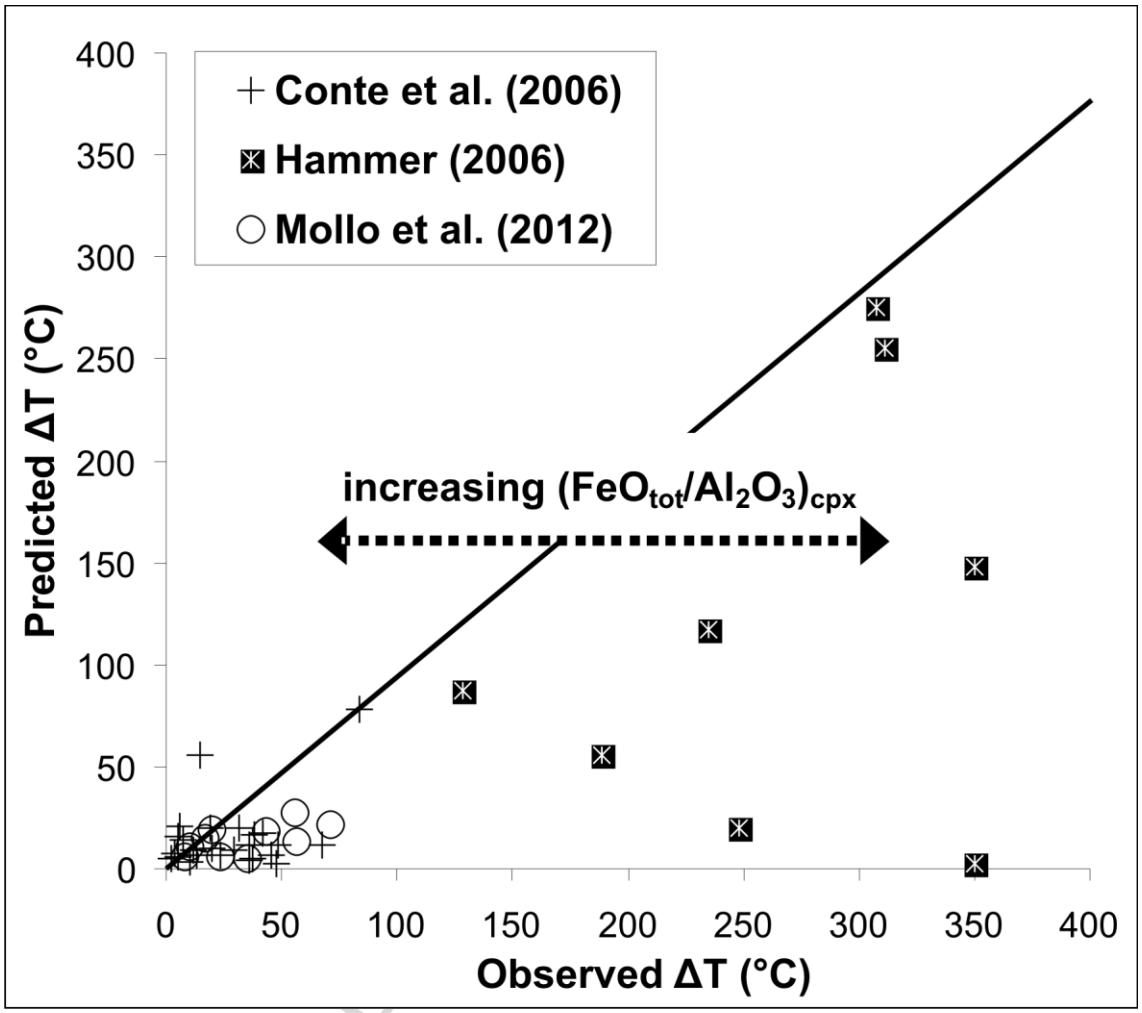

Fig. 8

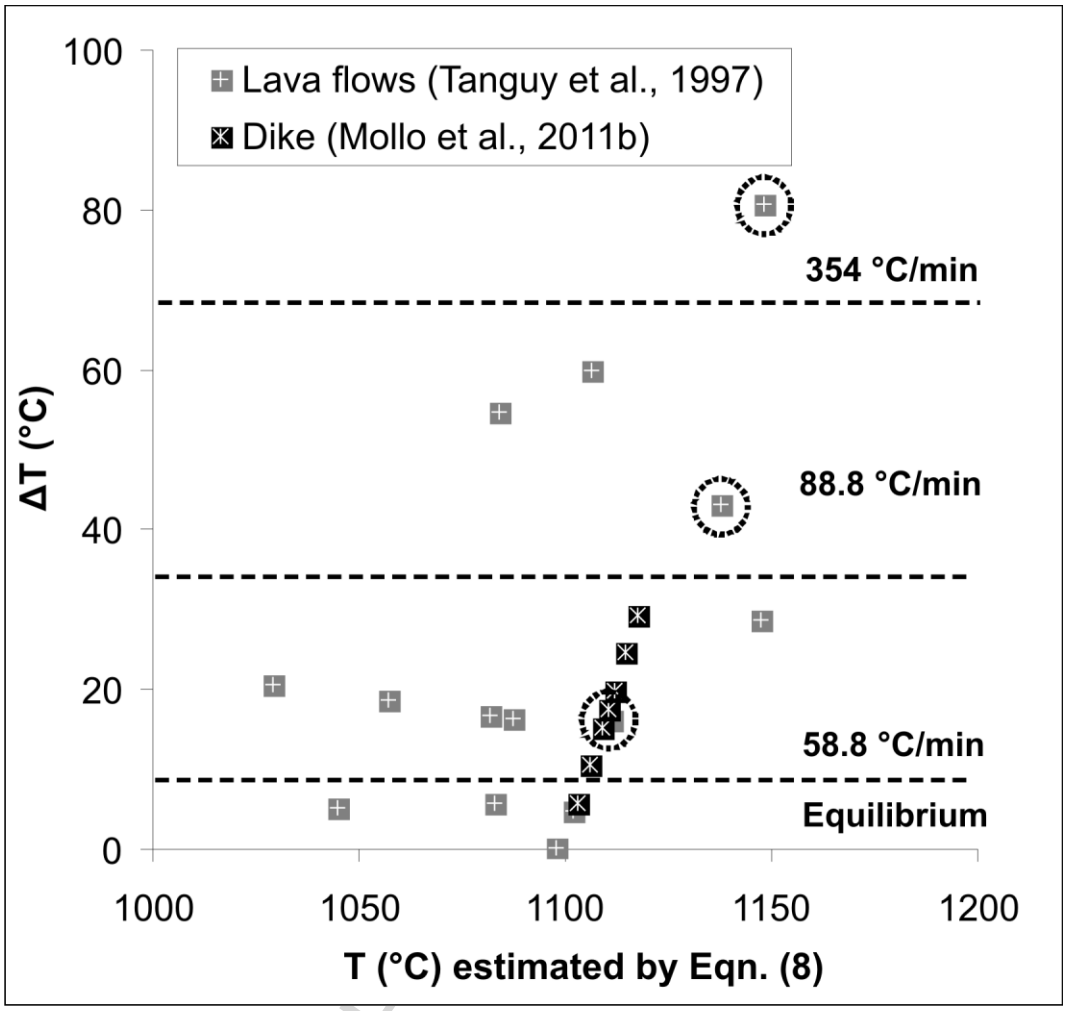

Fig. 9

Table 1. Run conditions and phases occurring in experimental products. Phase abundance was determined by mass balances. The sum of the squares of the residuals (SSR) does not exceed 0.29.

Run#	Cpx (wt.%)	Sp (wt.%)	Glass (wt.%)	Cooling rate (°C/h)	Final temperature (°C)	Buffer
Variable isothermal temperature						
VFEB01	-	-	100	-	1200	NNO+1.5
VFEB03	28	3	69	-	1100	NNO+1.5
VFEB04	-	-	100	-	1200	QFM
VFEB06	24	3	73	-	1100	QFM
Variable cooling rate						
VFEB07	21	3	76	2.5	1100	NNO+1.5
VFEB08	18	2	80	10	1100	NNO+1.5
VFEB09	11	2	87	50	1100	NNO+1.5
VFEB10	16	2	82	2.5	1100	QFM
VFEB11	10	1	89	10	1100	QFM
VFEB12	6	1	93	50	1100	QFM

Research Highlights

> Under rapid cooling rates clinopyroxenes do not equilibrate with the melt. > Consequently, thermometers predict higher crystallization temperatures. > This allows to estimate the solidification path of Etnean rocks.